Food Biophysics (2024) 19:688–700
https://doi.org/10.1007/s11483-024-09860-8

RESEARCH

Identification of Potential α-Glucosidase Inhibitors from American Ginseng Processed Products by UHPLC-Q-Orbitrap/MS and Molecular Docking

Liwen Liang[1] · Xiaokang Liu[1] · Juan Shao[1] · Jiaqi Shen[1] · Youzhen Yao[1] · Xin Huang[2] · Guangzhi Cai[1] · Yunlong Guo[2] · Jiyu Gong[1]

Received: 10 April 2024 / Accepted: 13 June 2024 / Published online: 18 June 2024

Abstract

The traditional herb American ginseng (*Panax quinquefolium* L.) can be processed into two common products: dried American ginseng (DAG) and red American ginseng (RAG), which have well-established hypoglycemic activity, making it a functional food as well. However, the mechanism by which the main active ingredients inhibit α-glucosidase, a crucial target for hypoglycemic drugs, remains unclear. In this research, we employed ultra-high-performance liquid chromatography coupled with quadrupole orbitrap mass spectrometry (UHPLC-Q-Orbitrap/MS) to analyze the chemical composition of ethanol extracts of dried American ginseng (EDAG) and red American ginseng (ERAG). Subsequent in vitro experiments were conducted to assess the α-glucosidase inhibitory activity of EDAG and ERAG. Comparative enzymatic kinetics analyses were performed as well. Molecular docking analysis revealed the interaction between the differential saponins and α-glucosidase, further validated through verification experiments. Among the total 47 identified saponins, 9 were characterized by OPLS-DA as differentially expressed between EDAG and ERAG. Notably, ERAG exhibited more robust α-glucosidase inhibitory activity than EDAG. Enzyme inhibition kinetics revealed that both products displayed reversible mixed-type inhibition on α-glucosidase, suggesting their inhibitory effects are associated with saponin composition. Molecular docking studies demonstrated that all 9 differential saponins exhibited inhibitory effects on α-glucosidase. Verification studies substantiated ginsenosides like Rb_1, Rd, and others as inhibitors of α-glucosidase. These findings contribute to a more comprehensive understanding of processed American ginseng and provide valuable insights for developing glucose-lowering functional foods.

Keywords American Ginseng · Inhibitors · α-Glucosidase · Molecular Docking

Introduction

American ginseng (*Panax quinquefolium* L.), a traditional medicine, originates from Canada and the United States. Since the 1980s, China has become the primary producer of American ginseng due to its extensive large-scale farming [1]. Currently, the main production regions of American ginseng in China are Shandong, Jilin, and Heilongjiang provinces [2]. American ginseng has pharmacological benefits, including antioxidation, anti-tumor, hypoglycemic, and hypolipidemic. It contains various active ingredients, including saponins, sugars, flavonoids, and volatile oils [3–5]. Additionally, American ginseng as medicinal and edible homologous resource, can be utilized as a tonic to create a variety of health foods, especially for elderly and frail people.

Diabetes mellitus is a chronic disease characterized by hyperglycaemia [6]. As of 2021, there were 529 million individuals diagnosed with diabetes globally, with a worldwide age-standardized diabetes prevalence of 6.1%. It is

Liwen Liang and Xiaokang Liu contributed equally to this work.

✉ Yunlong Guo
Guoyl02@ccucm.edu.cn

[1] School of Pharmaceutical Sciences, Changchun University of Chinese Medicine, Changchun 130117, China

[2] Jilin Ginseng Academy, Changchun University of Chinese Medicine, Changchun 130117, China

widely thought that by 2050, the global diabetic population will rise to 1.31 billion [7]. During the early stages of treatment, inadequate hyperglycemia control increases the risk of various diabetic complications, encompassing diabetic nephropathy, cardiovascular issues, neuropathy, and ocular and hepatic complications [8]. α-Glucosidase, a crucial enzyme in carbohydrate hydrolysis, plays a significant role in the process of food absorption. Inhibiting the activity of α-glucosidase can effectively lower postprandial blood glucose levels and help control the progression of diabetes [9]. At present, chemically synthesized α-glucosidase inhibitors are associated with notable side effects and discomfort [10]. These findings highlight the importance of the quest for safe α-glucosidase inhibitors with minimal toxic effects.

Natural products have emerged as pivotal resources in drug development, yielding valuable α-glucosidase inhibitors. The exploration and development of drugs from natural products, specifically those targeting α-glucosidase, have become focal points in new drug research. Existing studies underscore the hypoglycemic potential of several plant-derived active compounds, including saponins, evident in diverse diabetes models. For example, animal experiments revealed significant hypoglycemic and hypolipidemic activities in diabetic mice due to the total saponins of *Staunonia chinensis* [11]. In addition, oleanolide-type saponins in *Ligulariopsis shichuana* [12], steroidal saponins from *fenugreek* [13]and *platycodi radix* saponin [14]reportedly exhibit effective inhibition of α-glucosidase activity, thus reducing the blood sugar levels in diabetic patients.

American ginseng and Asian ginseng are two main plants of the genus Panax and have similar pharmacological effects [15]. Asian ginseng is steamed into red Asian ginseng. Compared with unsteamed Asian ginseng, red Asian ginseng has stronger biological activity. Moreover, it is debatable whether the biological activity of American ginseng changes like Asian ginseng after steaming. In recent years, American ginseng had two types of popular products by drying and steaming process, named dried American ginseng (DAG) and red American ginseng (RAG), respectively [16]. Previous reports mostly emphasized the influence of different processing methods on the chemical composition of American ginseng products, but there was limited research on its hypoglycemic effect.

Ginsenosides, recognized as primary bioactive components of DAG and RAG, particularly undergo chemical transformations during RAG's processing (involving steam treatment), yielding novel bioactive compounds absent in DAG [17]. For instance, DAG contains malonyl-ginsenosides featuring a malonyl residue linked to glucose, while this thermally unstable malonyl residue is hydrolyzed during steaming, yielding RAG and its rare ginsenosides. RAG exhibits more potent pharmacological effects than DAG. Moreover, distinct ginsenosides, such as Rg_3, Rk_3, and Rg_5, demonstrate varying bioactivities and clinical applications. Increased ginsenoside Rg_3 content in RAG has been associated with enhanced anti-proliferative effects [18], while ginsenoside Rk_3 and Rg_5 exhibit specific hypoglycemic effects in diabetic mice [19]. In addition, ginsenoside Re and Rb_2 in DAG were found to significantly mitigate weight changes, fat accumulation, and insulin resistance caused by high-fat diets in mice [20, 21]. However, it is not clear whether the main active components in these two processed products may have a hypoglycemic effect by inhibiting α-glucosidase.

This study employed ultra-high-performance liquid chromatography coupled with quadrupole Orbitrap mass spectrometry (UHPLC-Q-Orbitrap/MS) to elucidate the chemical composition of ethanol extracts of dried American ginseng (EDAG) and red American ginseng (ERAG). Subsequent multivariate statistical analysis revealed the primary differential saponins between EDAG and ERAG. α-Glucosidase incubation and enzyme kinetic experiments were conducted to differentiate the inhibitory activities of EDAG and ERAG. Additionally, molecular docking techniques were utilized to explore the docking effects of differential saponins from EDAG and ERAG on α-glucosidase. Experimental validation analysis of differential monomeric saponins was conducted for α-glucosidase inhibition.

Materials and Methods

Materials and Reagents

Chromatographic grade acetonitrile and methanol were obtained from Fisher Scientific (Pittsburgh, PA, USA). Formic acid in MS grade was acquired from Sigma-Aldrich (St. Louis, MO, USA). For standards, ginsenosides Re (B21055), Rg_1 (B21057), Rb_1 (B21050), Rg_2 (B21058), Rc (B21053), Rb_2 (B21051), Rd (B21054), Rg_6 (B27837), 20(R)-Rg_3 (B21759), Acarbose (B21003), α-glucosidase (Saccharomyces cerevisiae) and p-Nitrophenyl-α-D-glucopyranoside (pNPG) were obtained from Shanghai Yuanye Biotechnology Co. Ltd. (Shanghai, China).

Ten batches of American ginseng herbal materials were collected from the primary origin of American ginseng in Changbai mountain, China, and identified by Prof. Jiyu Gong of Changchun University of Chinese Medicine, School of Pharmaceutical Sciences.

Processed American Ginseng Samples

The fresh American ginseng samples were initially cleaned and subsequently processed involving drying and steaming procedures. The preparation of DAG entailed washing

fresh ginseng and subjecting it to hot air drying at 50°C. In contrast, the production of RAG involved steaming fresh ginseng roots at temperatures ranging from 95 to 100 °C for 3 h, followed by drying in an oven at 50°C.

Sample Solution Preparation

The EDAG and ERAG were obtained as follows. In detail, DAG and RAG samples were powdered using a pulverizer before extraction, the sample powder (100 g) was soaked in 1000 mL of 70% ethanol and extracted in a reflux condenser for 3 h. Lastly, the extract was evaporated on a rotary evaporator, concentrated by lyophilization, and then stored at -20 °C.

EDAG and ERAG powder (0.1 g) was ultrasonically extracted using 80% methanol-water (5 mL) for 15 min. The extraction was filtered through a 0.22 μm membrane filter. The filtrate was transferred into a sample vial for UHPLC-Q-Orbitrap/MS analysis.

UHPLC-Q-Orbitrap/MS Analysis

A Ultimate 3000 ultra-high-performance liquid chromatography system (Thermo, San Jose, CA, USA) was used for chromatographic separation. An Agilent C18 column (3.0 × 100 mm, 2.7 μm, Sigma-Aldrich) was maintained at 30°C for optimal separation. The mobile phases consisted of solvent A and solvent B, where solvent A was composed of water containing 0.1% formic acid, and solvent B was acetonitrile. The separation of experimental samples was carried out according to the following gradient elution program: 82–80% A (0–12 min), 80–70% A (12–14 min), 70–68% A (14–24 min), 68–67% A (24–29 min), and 67–25% A (29–50 min). The injection volume was set to 5 μL, and the flow rate was maintained at 0.5 mL/min.

A Q-Orbitrap-MS/MS (Thermo, San Jose, CA, USA) system was employed, utilizing an electrospray ionization (ESI) source operating in the negative ion mode. The ESI source parameters were configured as follows: sheath gas flow rate of 35 arbitrary units (Arb), auxiliary gas flow rate of 10 Arb, sweep gas flow rate of 1 Arb, capillary voltage set at -3.5 kV, and capillary temperature maintained at 350°C. Full MS data acquisition encompassed a scan range of m/z 150–2000 Da, employing a resolution of 70,000, an automatic gain control (AGC) target of 1×10^6, and a maximum injection time (IT) of 100 ms. For dd-MS^2 scans, a resolution of 17,000 was utilized, accompanied by an AGC target of 1×10^5, IT of 50 ms, loop count set at 5, isolation window of 4.0 m/z, and normalized collision energy (NCE) spanning from 35 to 55. Subsequently, Full MS/dd-MS^2 mode was implemented for the analytical procedure.

In Vitro Assay of α-Glucosidase Inhibition

Inhibition of α-glucosidase in vitro was analyzed according to a previously described method, with minor modifications [22]. 20 μL of various concentrations of the test samples were introduced into a 96-well plate. This was followed by the addition of 80 μL of 0.1 mol/L phosphate buffer (pH 6.8) and 20 μL of 0.3 U/mL α-glucosidase. After pre-incubation at 37°C for 15 min, the mixture was further supplemented with 20 μL of a 2.5 mmol/L substrate solution, pNPG. The resulting mixture was then incubated at 37°C for an additional 15 min. The reaction was stopped by adding 80 μL 0.2 mol/L Na_2CO_3. Absorbance was measured at 405 nm. Acarbose was adopted as a positive control. The assay was performed in triplicate.

The inhibition percentage was calculated as follows:

$$\text{Inhibition } (\%) = \left(1 - \frac{C - D}{A - B}\right) \times 100\ \% \quad (1)$$

where A, B, C, and D represent the absorbance of the control (enzyme and PBS), control blank (denatured enzyme and PBS), sample (enzyme and inhibitor), and sample blank (denatured enzyme and inhibitor), respectively. IC_{50} is defined as the amount of extracts required to inhibit 50% of α-glucosidase activity.

Enzyme Kinetics Assays

The same procedure outlined in the section on α-glucosidase inhibitory activity was replicated to investigate enzymatic inhibition kinetics. In essence, varying concentrations of the test samples (0, 1, 2, 3 mg/mL) were combined with a constant concentration of pNPG (2.5 mmol/L) and α-glucosidase at different concentrations (0.10, 0.15, 0.20, 0.25, 0.30, 0.35 U/mL) to ascertain the reversibility of the test samples' impact on α-glucosidase through graphical analysis.

Variable concentrations of tested samples (0, 1, 2, 3 mg/mL) were combined with varying pNPG concentrations (0.5, 1.0, 1.5, 2.0, 2.5, and 3.0 mmol/L) while maintaining a fixed α-glucosidase concentration (0.3 U/mL). A Lineweaver-Burk double reciprocal curve was plotted. The parameters were calculated by the following equation:

$$\frac{1}{V} = \frac{Km}{Vmax}\frac{1}{[S]} + \frac{1}{Vmax} \quad (2)$$

Where V: Reaction rate, V_{max}: Maximum reaction rate, K_m: Michaelis constant, [S]: Substrate concentration.

Molecular Docking

The crystalline α-glucosidase complex was obtained from the Protein Data Bank (http://www.rcsb.org). Water molecules and proto-ligands were removed utilizing the PyMOL software suite. The resultant structure was saved in PDB format and subsequently subjected to processes including hydrogenation and charge calculation using AutodockTools 1.5.7, resulting in the PDBQT format. The three-dimensional structure of ginsenoside was constructed using ChemBio3D Ultra 14.0 software. AutodockTools 1.5.7 was employed to refine the structure, and the final version was saved in PDBQT format for archival purposes. Binding processes were visually analyzed with the aid of PyMOL software. Parameters, such as binding energy, were extracted from the docking results to evaluate the interactions.

Statistical Analysis

The UHPLC-Q-Orbitrap/MS data were subjected to analysis using Sieve software (version 2.1, Thermo, San Jose, CA, USA) for peak extraction, alignment, and normalization. Subsequently, the datasets underwent multivariate analysis using SIMCA-P software (Umetrics, Umea, Sweden) to identify marker compounds responsible for the differences between EDAG and ERAG. The principal component analysis (PCA) model was established first to perform pattern recognition and obtain an overview of sample classification, followed by the orthogonal partial least-squares discriminant analysis (OPLS-DA) model to obtain the most significant separation among groups. Components with Variable Importance for the Projection (VIP) values exceeding 1 and a significance level of $p < 0.05$ were chosen as analytical markers in the OPLS-DA. The results were presented as mean ± SD of triplicate measurements. For the IC_{50} analysis of α-glucosidase inhibition and mapping, GraphPad Prism 9.0 software (GraphPad Prism Software, San Diego, CA) was employed.

Results

Analysis of the Chemical Composition of EDAG and ERAG Using UHPLC-Q-Orbitrap/MS

UHPLC-Q-Orbitrap/MS was used to analyze the chemical composition of EDAG and ERAG. The base peak intensity (BPI) chromatogram of EDAG and ERAG in negative ion mode is shown in Fig. 1. Subtle variations in peaks were discernible between EDAG and ERAG, indicating distinct chemical compositions. A comprehensive identification of 47 saponins was accomplished, comprising 23 protopanaxadiol (PPD) types, 10 protopanaxatriol (PPT) types, 3 oleanane (OA) types, 2 octolone (OT) types, and 9 C17-side chain variants. The detailed list of identified compounds from the two American ginseng processed products is presented in Table 1. This identification was achieved by cross-referencing the detected compounds' MS and MS/MS information with databases, literature sources, and standard references.

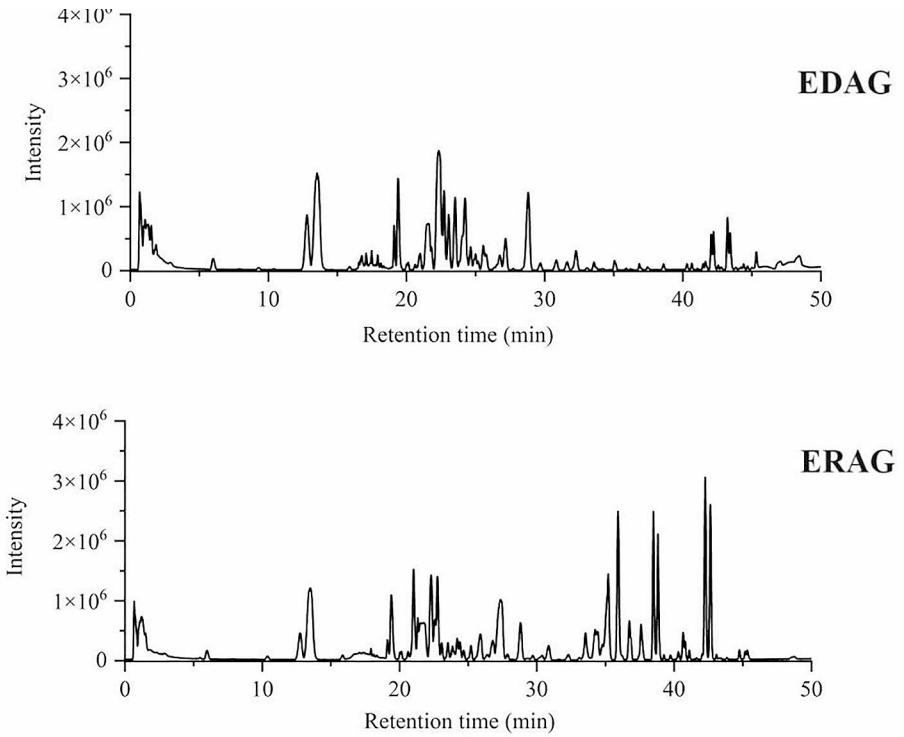

Fig. 1 The representative base peak intensity (BPI) chromatograms of two American ginseng processed products in negative ion mode

Table 1 Compounds identified from EDAG and ERAG by UHPLC-Q-Orbitrap/MS.

Compound	RT (min)	Identity	Formula	Detected m/z	Adducts	Mass Error (ppm)	Fragment ion	Type
1	8.00	Quinquenoside F_6	$C_{47}H_{80}O_{18}$	977.5362	$[M+HCOO]^-$	4.19	931.5325,799.4878,637.4302,	PPT
2	9.52	Noto-ginsenoside R_1	$C_{47}H_{80}O_{18}$	977.5362	$[M+HCOO]^-$	4.19	931.5277,799.4904,637.4351, 161.045	PPT
3	12.72	Ginsenoside Rg_1	$C_{42}H_{72}O_{14}$	845.4930	$[M+HCOO]^-$	3.78	799.4985,637.4350,475.3815, 416.5321	PPT
4	13.44	Ginsenoside Re	$C_{48}H_{82}O_{18}$	991.5535	$[M+HCOO]^-$	5.85	945.5467,793.4359,731.4450, 637.4425,475.3863	PPT
5	15.95	Quinquenoside L_{11}	$C_{42}H_{72}O_{14}$	799.4952	$[M-H]^-$	1.13	845.4954,654.1112	C17 side-chain varied
6	16.74	Malonyl-ginsenoside Rg_1	$C_{45}H_{74}O_{17}$	885.4907	$[M-H]^-$	6.78	841.5006,654.1274	PPT
7	17.04	Malonyl-ginsenoside Re	$C_{51}H_{84}O_{21}$	1031.5497	$[M-H]^-$	6.88	945.5435,637.4351,475.3798	PPT
8	17.80	Quinquenoside F_3	$C_{54}H_{94}O_{24}$	1125.6094	$[M-H]^-$	3.82	963.5545,801.5054,	C17 side-chain varied
9	17.84	Quinquenoside L_{14}	$C_{47}H_{80}O_{17}$	961.5418	$[M+HCOO]^-$	5.41	915.5337,783.4901	PPD
10	17.88	Quinquenoside IV	$C_{54}H_{90}O_{24}$	1167.5837	$[M+HCOO]^-$	2.14	1121.5795,959.5195,797.4725	PPD
11	18.19	Majoroside F_5	$C_{48}H_{82}O_{19}$	1007.5469	$[M+HCOO]^-$	4.27	961.5405,815.4818,799.4872, 653.4294	PPD
12	18.37	Majoroside F_1	$C_{48}H_{82}O_{19}$	1007.5469	$[M+HCOO]^-$	4.27	961.5399,781.4786,637.4354, 475.3813	C17 side-chain varied
13	19.08	Majonoside R_2	$C_{41}H_{70}O_{14}$	831.4779	$[M+HCOO]^-$	4.45	785.4688,767.4367,654.2980	OT
14	19.38	PseudoginsenosideF_{11}	$C_{42}H_{72}O_{14}$	845.4947	$[M+HCOO]^-$	5.80	799.4886,653.4321,491.3787, 398.2747	OT
15	19.97	Noto-ginsenoside R_2	$C_{41}H_{70}O_{13}$	815.4830	$[M+HCOO]^-$	5.27	769.4771,637.4362,475.3817	PPT
16	20.97	Ginsenoside Rg_2	$C_{42}H_{72}O_{13}$	829.5001	$[M+HCOO]^-$	6.27	783.4955,675.4850,637.4327, 475.3815	PPT
17	21.03	Ginsenoside Rh_1	$C_{36}H_{62}O_9$	683.4393	$[M+HCOO]^-$	3.37	475.3802	PPT
18	21.44	Ginsenoside Rb_1	$C_{54}H_{92}O_{23}$	1153.6078	$[M+HCOO]^-$	6.33	1107.5995,945.5510,621.4410, 458.7734	PPD
19	22.18	Malonyl-ginsenoside Rb_1	$C_{57}H_{94}O_{26}$	1193.6021	$[M-H]^-$	5.53	1107.6008,945.5478,783.4942, 621.4407	PPD
20	22.42	Ginsenoside Rc	$C_{53}H_{90}O_{22}$	1123.5962	$[M+HCOO]^-$	5.52	1077.5891,945.5446,783.4984, 621.4399,453.3906	PPD
21	22.84	Ginsenoside Ro	$C_{48}H_{76}O_{19}$	955.4930	$[M-H]^-$	2.93	793.4395,613.3684,569.3834	OA
22	23.56	Malonyl-ginsenoside Rc	$C_{56}H_{92}O_{25}$	1163.5889	$[M-H]^-$	3.44	1119.5975,945.5444,783.4922	PPD
23	23.73	Malonyl-ginsenoside Rb_2	$C_{56}H_{92}O_{25}$	1163.5889	$[M-H]^-$	3.44	1077.5878,945.5417,783.4972, 621.4399	PPD
24	23.79	Ginsenoside Rb_3	$C_{53}H_{90}O_{22}$	1123.5962	$[M+HCOO]^-$	5.52	1077.5859,945.5475,783.4837, 621.4343,459.3564	PPD
25	24.30	Ginsenoside Rb_2	$C_{53}H_{90}O_{22}$	1123.5963	$[M+HCOO]^-$	5.61	1077.5898,783.4940,621.4401,45 9.3871	PPD
26	25.90	Quinquenoside R_1	$C_{56}H_{94}O_{24}$	1195.6176	$[M+HCOO]^-$	5.44	1107.6005,1149.6108,945.5450, 987.5576,783.4950	PPD
27	26.74	Chikusetsu saponin II	$C_{42}H_{66}O_{14}$	793.4409	$[M-H]^-$	5.17	631.3876,613.3792,569.3867,	OA
28	27.20	Ginsenoside Rd	$C_{48}H_{82}O_{18}$	991.5530	$[M+HCOO]^-$	5.35	945.5461,783.4921,621.4406, 459.3887	PPD
29	28.08	GinsenosideRs_1/Rs_2	$C_{55}H_{92}O_{23}$	1119.5994	$[M-H]^-$	4.38	1077.5892,945.5471,783.4911,62 1.4435	PPD
30	28.12	Notoginsenoside Fc	$C_{55}H_{92}O_{23}$	1165.6038	$[M+HCOO]^-$	2.75	1077.5833,945.5497,783.4906,62 1.4366	PPD

Table 1 (continued)

Compound	RT (min)	Identity	Formula	Detected m/z	Adducts	Mass Error (ppm)	Fragment ion	Type
31	28.67	Malonyl-ginsenoside Rd	C51H84O_{21}	1031.5497	$[M-H]^-$	6.88	987.5612,945.5461,783.4941, 621.4387,459.3865	PPD
32	34.37	Noto-ginsenoside Fe	$C_{47}H_{80}O_{17}$	961.5418	$[M+HCOO]^-$	4.78	915.5357,783.4933,621.4380,	PPD
33	35.18	Ginsenoside Rg_6	$C_{42}H_{70}O_{12}$	811.4898	$[M+HCOO]^-$	6.78	765.4847,654.0493,423.7911	C17 side-chain varied
34	36.01	Ginsenoside Rg_4	$C_{42}H_{70}O_{12}$	811.4881	$[M+HCOO]^-$	2.46	765.4818,619.4234	PPT
35	37.37	Chikusetsu saponin III	$C_{47}H_{80}O_{17}$	915.5336	$[M-H]^-$	2.73	783.4935,621.4390,459.3850	PPD
36	37.52	Chikusetsu saponin Ib	$C_{47}H_{74}O_{18}$	925.4843	$[M-H]^-$	5.83	793.441,731.4401,569.3856, 455.3544	OA
37	38.38	20(R)-Ginsenoside Rg_3	$C_{42}H_{72}O_{13}$	829.5007	$[M+HCOO]^-$	6.99	783.4932,621.4392,459.3877	PPD
38	38.49	Ginsenoside F_2	$C_{42}H_{72}O_{13}$	783.4912	$[M-H]^-$	2.04	621.4360,459.3856	PPD
39	38.87	20(S)-Ginsenoside Rg_3	$C_{42}H_{72}O_{13}$	829.5002	$[M+HCOO]^-$	6.39	783.4948,621.4463,459.3874	PPD
40	40.63	Ginsenoside Rh_2	$C_{36}H_{62}O_8$	667.4470	$[M+HCOO]^-$	7.34	631.3875,455.3534	PPD
41	40.86	Ginsenoside 20(S) Rs_3	$C_{44}H_{74}O_{14}$	871.5054	$[M+HCOO]^-$	-0.11	783.4922,621.4381,459.3871	PPD
42	41.21	Ginsenoside 20(R) Rs_3	$C_{44}H_{74}O_{14}$	871.5054	$[M+HCOO]^-$	-0.11	783.4833,621.4375,459.3862	PPD
43	42.21	Ginsenoside Rk_1	$C_{42}H_{70}O_{12}$	811.4894	$[M+HCOO]^-$	6.28	765.4842,603.4290,161.0457	C17 side-chain varied
44	42.58	Ginsenoside Rg_5	$C_{42}H_{70}O_{12}$	811.4895	$[M+HCOO]^-$	6.41	765.4829,603.4292,161.0457	C17 side-chain varied
45	44.69	Ginsenoside Rs_5	$C_{44}H_{72}O_{13}$	853.5007	$[M+HCOO]^-$	6.80	807.4976,765.4807,654.1440	C17 side-chain varied
46	45.27	Ginsenoside Rs_4	$C_{44}H_{72}O_{13}$	853.5006	$[M+HCOO]^-$	6.68	765.4835,654.0742	C17 side-chain varied
47	47.60	Ginsenoside Rk_2	$C_{36}H_{60}O_7$	649.4350	$[M+HCOO]^-$	5.39	603.3433,161.0458	C17 side-chain varied

Multivariate Analysis for Distinguishing EDAG and ERAG

Unsupervised PCA analyses were conducted on raw EDAG and ERAG data to obtain a more distinct metabolite profile. As depicted in Fig. 2A, the PCA score plot illustrates the clustering of QC samples at the center, reflecting the experimental process and data collection stability. Notably, samples could be clearly separated into two groups on the PCA score plot. Each sample group was concentrated within class 1, indicating high repeatability within groups. A clear separation between the two groups showed significant alterations in American ginseng composition between the processed products.

For an in-depth exploration of differential components, a supervised OPLS-DA analysis model was adopted. As illustrated in Fig. 2B, the samples within each group were clearly separated and distributed on opposing sides without overlap. The calculated R^2Y and Q^2 values were determined as 0.986 and 0.997, respectively, indicating robust model explanatory and predictive capacities. Additionally, a permutation test ($n = 200$) was executed to validate the model, revealing permutated R^2 and Q^2 values (Fig. 2C) lower than the original values, confirming the absence of overfitting in the established model.

S-plot (Fig. 2D) and VIP value were used to identify differential compounds. A total of 170 ions were identified with a VIP value > 1.0. The t-test was used to evaluate the significance of these characteristic changes, and the compounds with statistical significance ($p < 0.05$) were finally selected as marker compounds. A total of 9 differential components were identified, including 20(R)-ginsenoside Rg_3,

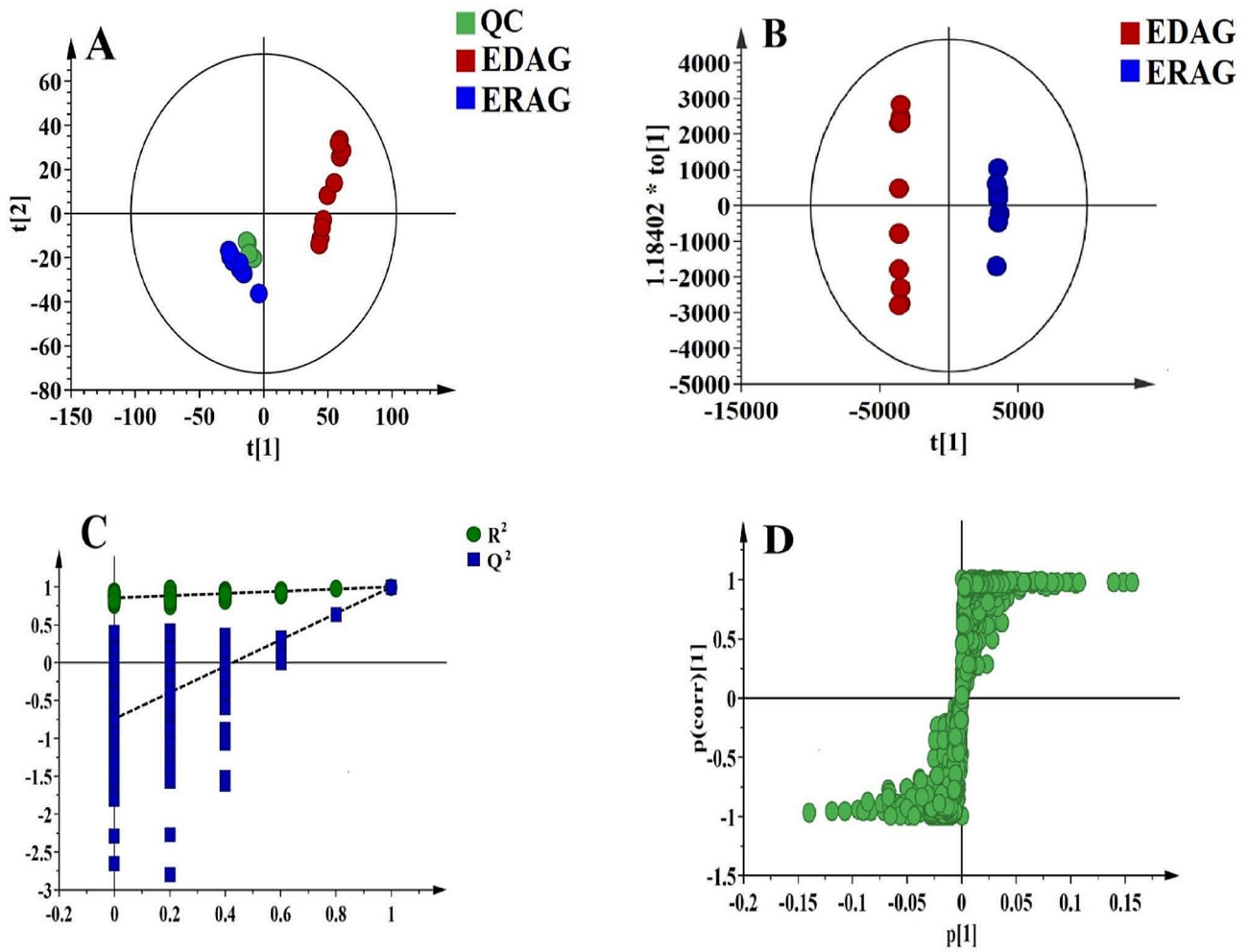

Fig. 2 PCA sore plot **(A)**, OPLS-DA score plot **(B)**, permutation test **(C)** and S-plot **(D)** of two American ginseng processed products

ginsenoside Rb_1, ginsenoside Rb_2, ginsenoside Rd, ginsenoside Re, ginsenoside Rg_1, ginsenoside Rg_6, ginsenoside Rc, and ginsenoside Rg_2. Among these, the relative content of ginsenoside Rg_1 and ginsenoside Re exhibited significant decreases in ERAG, whereas the other components exhibited a significant increase, as shown in Fig. 3.

α-Glucosidase Inhibitory Activity of EDAG and ERAG

The α-glucosidase inhibitory activity of EDAG, ERAG, and acarbose are shown in Fig. 4. Both EDAG and ERAG exhibited concentration-dependent α-glucosidase inhibition. The results revealed that the α-glucosidase inhibitory activity of EDAG and ERAG was correlated with the species and content of saponins. The inhibition rate demonstrated an initial increasing trend. Nevertheless, upon reaching a specific threshold, further increments in concentration ceased to produce additional changes in the inhibition rate, signifying the curve's stabilization.

For reflecting the α-glucosidase inhibitory activity, the IC_{50} values were calculated for EDAG (1.14 ± 0.4 mg/mL), ERAG (0.78 ± 0.2 mg/mL), and acarbose (17.53 ± 0.79 ng/mL) (Table 2). Lower IC_{50} values were associated with more potent inhibition. While distinct from acarbose, the inhibitory effects of EDAG and ERAG were consistent with those of other natural compounds [23, 24]. Notably, the α-glucosidase inhibitory effect of ERAG was twofold that of EDAG, attributed to their differences in active components.

Analysis of the Mechanism of α-Glucosidase Inhibition by EDAG and ERAG

The reversible inhibition experiments of EDAG and ERAG on α-glucosidase are shown in Fig. 5A and B. The linear nature of the lines, passing through the origin, coupled with the gradual slope decrease as EDAG and ERAG concentrations increased, indicated that both samples exhibited decreased enzyme catalytic activity in a reversible manner.

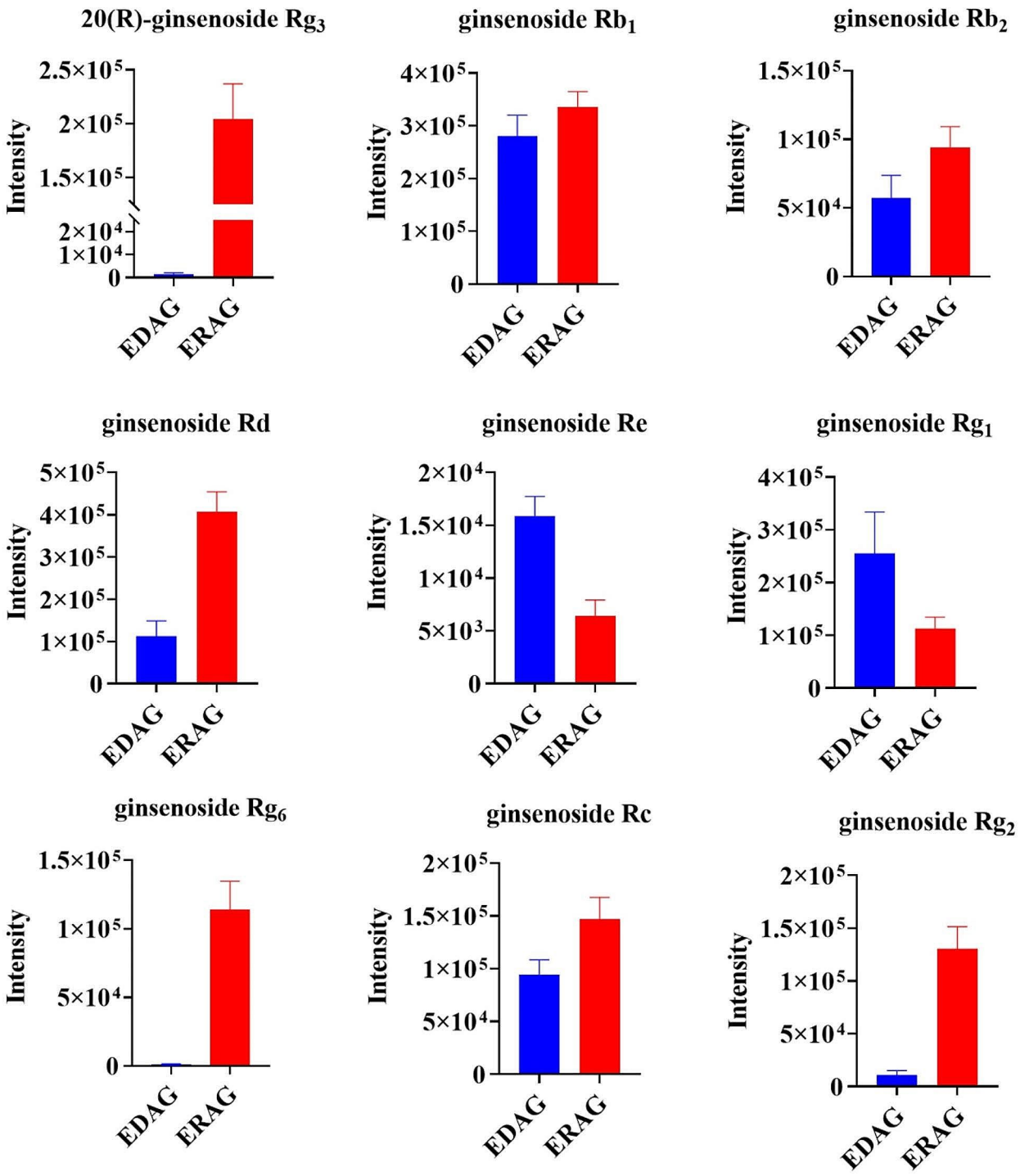

Fig. 3 Comparison of the total ion intensity of EDAG and ERAG.

Enzyme kinetic parameters were used to deduce the inhibition type, supported by the enzyme kinetic curves of EDAG and ERAG presented in Fig. 5C and D. The Lineweaver-Burk plot revealed a linear correlation between 1/V and 1/pNPG.

The maximum enzyme velocity (V_{max}) and Michaelis constant (K_m) values for α-glucosidase inhibition by EDAG and ERAG were calculated from Eq. (2). As shown in Table 3, increasing inhibitor concentrations led to diminished V_{max} and K_m values, in line with the characteristics of

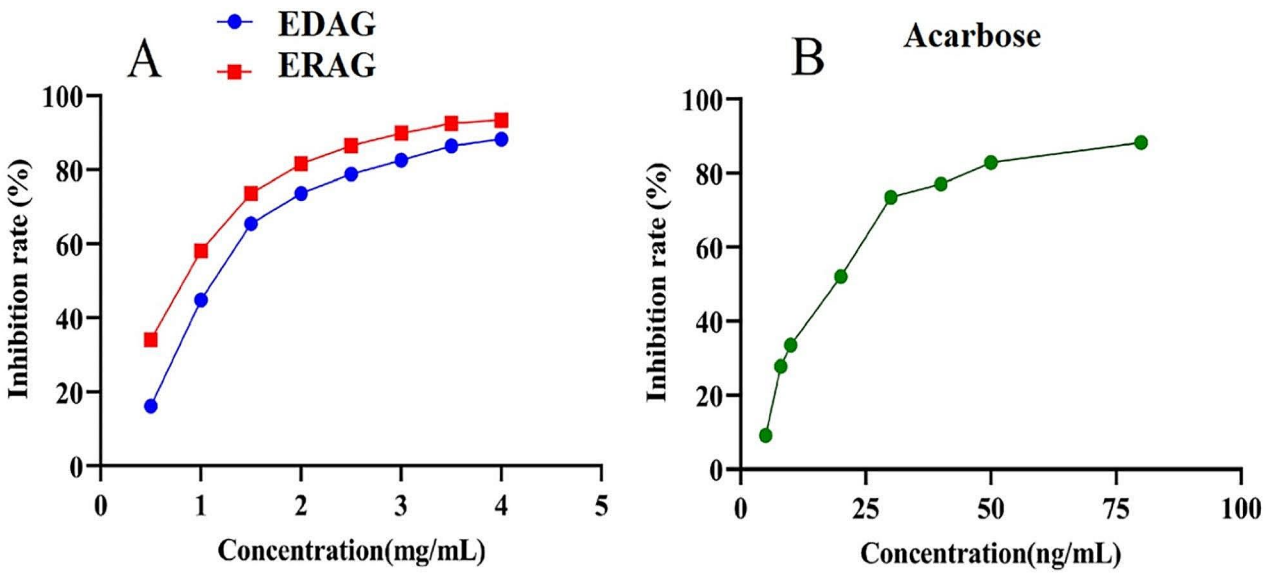

Fig. 4 Inhibitory effect of EDAG, ERAG **(A)** and acarbose **(B)** on the activity of α-glucosidase (The results shown are means ± SD, $n = 10$)

Table 2 Inhibitory activity of EDAG and ERAG on α-glucosidase ($n = 10$)

Sample	IC_{50} value
EDAG	1.14 ± 0.4 mg/mL
ERAG	0.78 ± 0.2 mg/mL
Acarbose	17.53 ± 0.79 ng/mL

mixed inhibitors. Notably, ERAG exhibited both a smaller K_m value and stronger α-glucosidase inhibitory activity than EDAG.

Molecular Docking Screening of Potential Inhibitors of EDAG and ERAG

LC-MS revealed 9 differential components within EDAG and ERAG. Given the observed significant differences in α-glucosidase inhibition, a molecular docking approach was applied to assess the α-glucosidase activities of these 9 components. Molecular docking is a theoretical simulation method used to study the interactions between molecules (such as ligands and receptors), predict their binding modes, and assess their affinity. It involves spatial and energy matching between molecules. The lower the binding energy, the more stable the docking conformation, indicating stronger binding between the active ingredient and the protein, and better affinity. As indicated in Table 4, all 9 compounds exhibited lower binding energies, suggesting stable conformation within the docking structure. The interactions between the screened compounds and α-glucosidase were elucidated through molecular docking, showcased in Fig. 6. Remarkably, ginsenoside Rb_1, ginsenoside Rd, ginsenoside Rb_2, and ginsenoside Rc demonstrated binding energies below −8.5, which indicates that they have high stability and affinity among proteins, and their inhibitory ability on α -glucosidase is outstanding among the nine different components. Additionally, ginsenoside Rb_1 displayed potentially higher inhibitory activity, while ginsenoside Rc exhibited weaker inhibition.

In Vitro Analysis of the Potential α-Glucosidase Inhibitory Activity Among Potential Ginsenosides

Molecular docking highlighted 9 differential saponins as potential α-glucosidase inhibitors. This section verified the inhibitory activities against α-glucosidase for bioactive saponins, specifically ginsenoside Rd, ginsenoside Rb_1, ginsenoside Rb_2, and ginsenoside Rc. All four differential saponins demonstrated inhibitory effects on α-glucosidase, albeit with varying potency (Table 5). Ginsenoside Rb_1 exhibited the highest α-glucosidase inhibition at identical concentrations with a molecular docking binding energy of -8.8. In contrast, ginsenoside Rc displayed the weakest inhibition with a molecular docking binding energy of -8.6. These findings are consistent with those of enzyme assays, validating the reliability of molecular docking and the classification of all 9 differential saponins as α-glucosidase inhibitors.

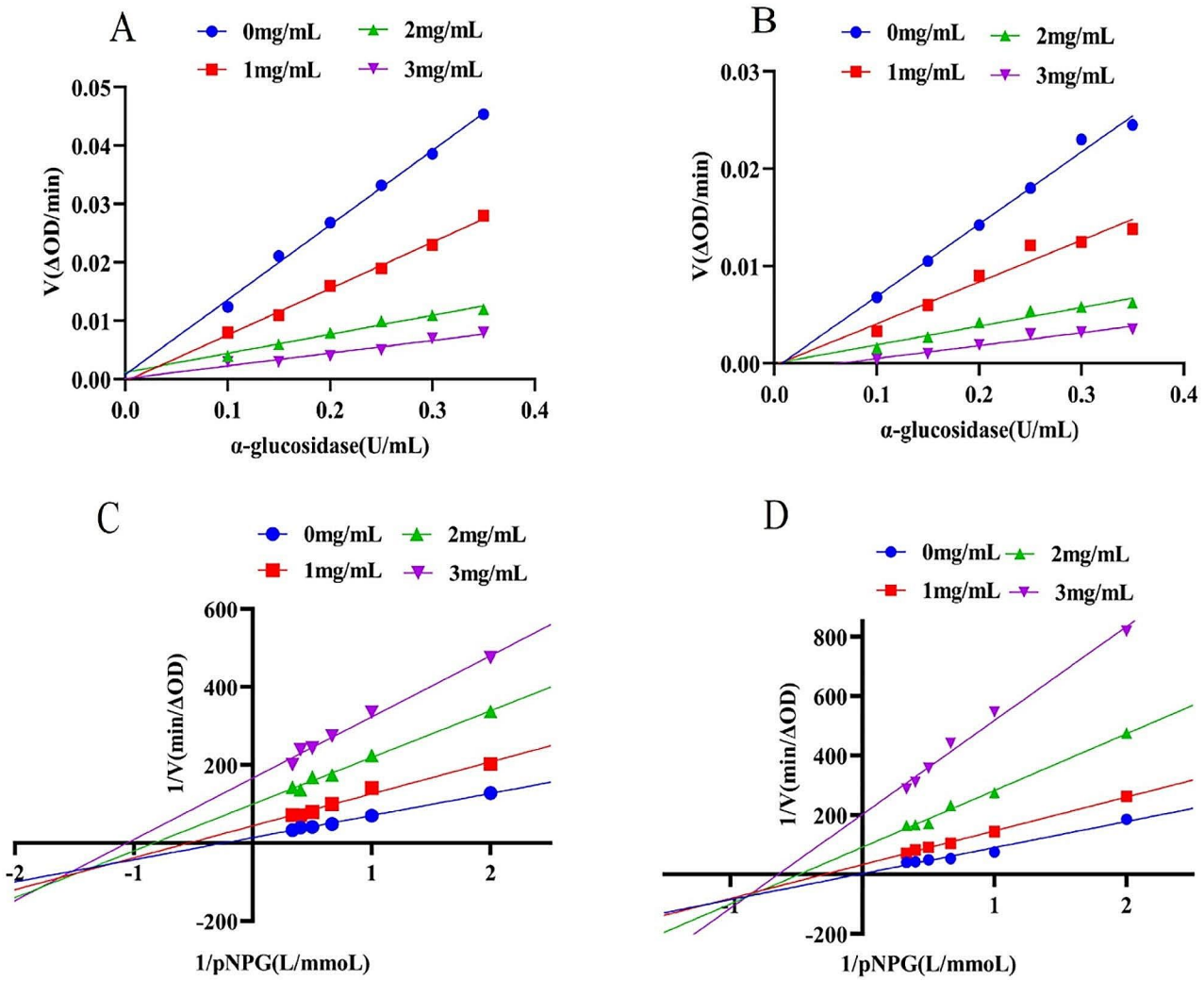

Fig. 5 Enzyme kinetic inhibition plots of α-glucosidase inhibition by EDAG and ERAG. Reversible test of EDAG **(A)** and ERAG **(B)** on the activity of α-glucosidase; Lineweaver – Burk plots of EDAG **(C)** and ERAG **(D)** on the activity of α-glucosidase

Table 3 V_{max} and K_m values of EDAG and ERAG inhibition of α-glucosidase

	Inhibitor Concentration (mg/mL)	K_m	V_{max}
EDAG	0	30.38 ± 0.35	0.356 ± 0.005
	1	3.41 ± 0.06	0.032 ± 0.002
	2	2.08 ± 0.04	0.016 ± 0.005
	3	1.58 ± 0.01	0.005 ± 0.001
ERAG	0	4.16 ± 0.29	0.071 ± 0.002
	1	1.82 ± 0.09	0.023 ± 0.001
	2	1.21 ± 0.03	0.016 ± 0.005
	3	0.93 ± 0.06	0.006 ± 0.001

Table 4 Binding energy of the potential bioactive compounds

Compounds	Binding energy (Kcal/mol)
20(R)-Ginsenoside Rg_3	-8.2
Ginsenoside Rb_1	-8.8
Ginsenoside Rb_2	-8.7
Ginsenoside Rg_1	-7.6
Ginsenoside Rc	-8.6
Ginsenoside Rd	-8.7
Ginsenoside Rg_2	-8.1
Ginsenoside Re	-7.5
Ginsenoside Rg_6	-8.0
Acarbose	-7.9

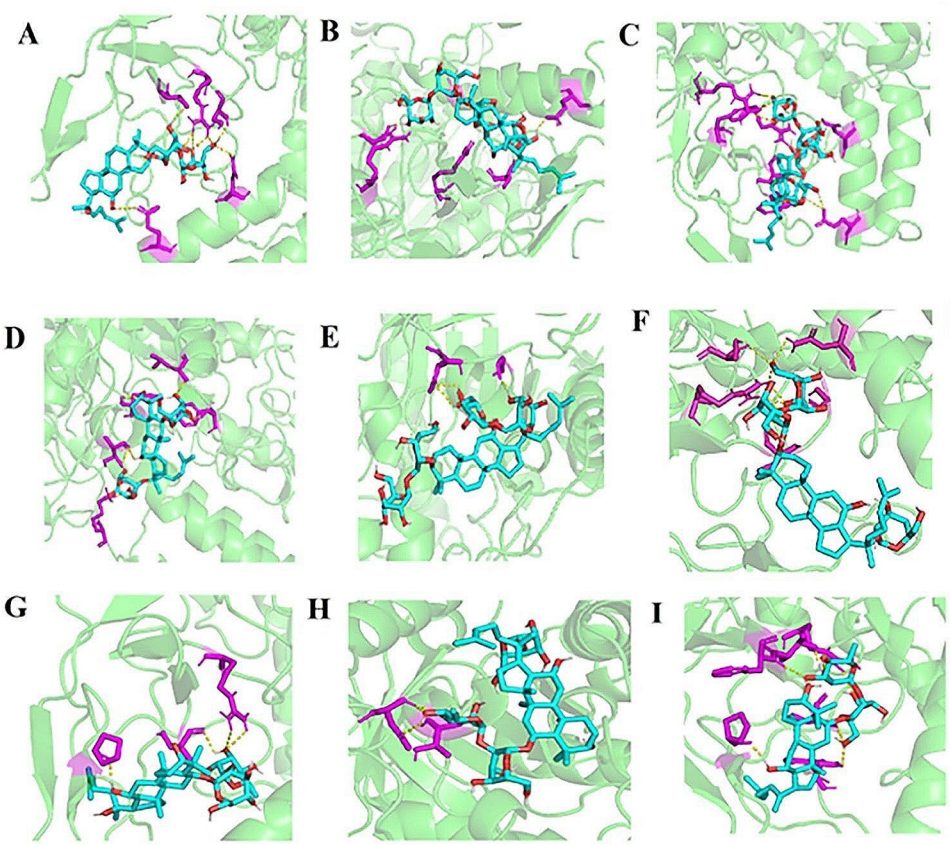

Fig. 6 Docking poses of the interactions between the screened inhibitors of α-glucosidase. **A**: 20(R)-Ginsenoside Rg_3, **B**: Ginsenoside Rb_1, **C**: Ginsenoside Rb_2, **D**: Ginsenoside Rg_1, **E**: Ginsenoside Rc, **F**: Ginsenoside Rd, G:Ginsenoside Rg_2, **H**: Ginsenoside Re, **I**: Ginsenoside Rg_6

Table 5 Inhibitory effects of ginsenosides on the activity of α-glucosidase

Sample	Concentration (mg/mL)	Inhibition rate (%)
Ginsenoside Rd	5	36.56 ± 0.51
	3	23.66 ± 0.23
	1	11.80 ± 0.42
Ginsenoside Rb_1	5	45.01 ± 0.69
	3	28.32 ± 0.29
	1	17.64 ± 0.51
Ginsenoside Rc	5	12.23 ± 0.57
	3	6.79 ± 0.68
	1	3.89 ± 0.81
Ginsenoside Rb_2	5	16.78 ± 0.47
	3	7.83 ± 0.81
	1	5.21 ± 0.52

Discussion

In this investigation, American ginseng, a well-known Chinese herbal remedy, was investigated for its essential active components, the saponin compounds. Previous studies have highlighted the impact of steaming on American ginseng, leading to structural conversions in ginsenosides. Steaming methods can decrease ginsenoside Re and ginsenoside Rg_1 content while enhancing rare ginsenosides like Rg_3 and ginsenoside CK, ultimately boosting efficiency [25, 26]. The current study identified 47 saponins and employed multivariate statistical analysis to identify 9 differential saponins between EDAG and ERAG. Notably, significant decreases in ginsenoside Re and Rg_1 content post-steaming were attributed to sugar chain cracking in ginsenosides. Moreover, three rare ginsenosides, including 20(R)-ginsenoside Rg_3, ginsenoside Rg_6, and ginsenoside Rk_1, were characterized in ERAG.

In recent years, many studies have shown that saponins of traditional Chinese medicine can effectively prevent and treat diabetes [27]. Effective control of blood sugar levels is crucial in managing type 2 diabetes. Ginsenosides can be effectively absorbed and metabolized in the digestive tract, and have the functions of restoring intestinal immune disorder, repairing damaged mucosal integrity, and reducing intestinal flora dysfunction [28]. In addition, the total saponin of American ginseng stems and leaves acts on the brush border of the small intestine in rats and has a limited effect on fatty acid absorption in this part [29]. α-Glucosidase inhibitors play a pivotal role in reducing carbohydrate absorption by inhibiting α-glucosidase within the small intestine's brush border, leading to decreased postprandial blood glucose [10]. Interestingly, this study revealed

superior α-glucosidase inhibitory activity in ERAG compared to EDAG, attributed to differences in saponin species and content after steaming. Furthermore, the study indicated reversible inhibition for EDAG and ERAG, with a mixed inhibition type that aligns with blueberry leaf polyphenols' inhibition pattern [30]. While EDAG and ERAG exhibit effective natural α-glucosidase inhibition, further confirmation through in vivo experiments is necessary. It is highly conceivable that this inhibitory effect extends to α-glucosidase from sources other than *Saccharomyces cerevisiae*, the source used in this study.

Molecular docking can predict whether binding and binding forces occur between small molecular ligands and receptor proteins. Herein, the molecular docking of 9 different compounds with α-glucosidase was studied. The anti-α-glucosidase activities of ginsenoside Rd, Rb_1, Rb_2, and Rc were examined, validating ginsenoside Rd's robust inhibitory effect, consistent with prior findings [21]. While ginsenoside Rb_1 and ginsenoside Rd, which experienced considerable changes pre- and post-steaming, demonstrated potent α-glucosidase inhibition, a gap persisted compared to EDAG and ERAG. This discrepancy might stem from the complexity of total saponins versus individual ginsenosides, with multiple components potentially working synergistically for a more potent inhibitory effect.

Conclusion

This study identified 47 saponins in EDAG and ERAG using UHPLC-Q-Orbitrap/MS, encompassing 23 PPD-types, 10 PPT-types, 3 OA-types, 2-OT types, and 9 C17-side chain variants. A comprehensive multivariate statistical analysis identified 9 differential saponins across the two American ginseng processed products. In vitro assessments substantiated ERAG's superior α-glucosidase inhibitory activity over EDAG. Enzyme inhibition kinetics supported reversible mixed-type inhibition for both products, underscoring their α-glucosidase inhibitory effects correlated with saponin composition. Furthermore, molecular docking investigations unveiled inhibitory effects for all 9 differential saponins on α-glucosidase. Validation analysis confirmed ginsenosides Rb_1, Rd, and others as α-glucosidase inhibitors. These findings contribute to a more comprehensive understanding of processed American ginseng and provide valuable insights for developing glucose-lowering functional foods.

Acknowledgements This work was supported by The National Natural Science Foundation of China (No. 81903778); The China National Traditional Chinese Medicine Standardization Project (No. ZYBZH-Y-JL-25) and The Science and Technology Development Plan Project of Jilin Province (No 20200201196JC).

Author Contributions Liwen Liang : Conceived and designed the experiment, analyzed the data and wrote the manuscript.Xiaokang Liu: Performed the format of the manuscript.Juan Shao : Contributed the manuscript language. Jiaqi Shen : Supervised the study and helped to initiate the project. Youzhen Yao : Supervised the study and helped to initiate the project.Xin Huang: Supervised the study and helped to initiate the project.Guangzhi Cai : Supervised the study and helped to initiate the project.Yunlong Guo: Supervised the study and helped to initiate the project. Jiyu Gong : Supervised the study and helped to initiate the project.

Data Availability No datasets were generated or analysed during the current study.

Declarations

Competing Interests The authors declare no competing interests.

References

1. L. Yang, Q. Yu, Y. Ge, W. Zhang, Y. Fan, C. Ma, Q. Liu, L. Qi, Distinct urine metabolome after Asian ginseng and American ginseng intervention based on gc-ms metabolomics approach. Sci. Rep. **6**, 39045 (2016)
2. Z. Li, Z. Shao, D. Qu, X. Huo, M. Hua, J. Chen, Y. Lu, J. Sha, S. Li, Y. Sun, Transformation mechanism of rare ginsenosides in American ginseng by different processing methods and antitumour effects. Front. Nutr. **9**, 833859 (2022)
3. L. Qi, C. Wang, C. Yuan, Ginsenosides from American ginseng: chemical and pharmacological diversity. Phytochemistry. **72**, 689–699 (2011)
4. H. Tang, X. Wang, J. Li, J. Zhang, C. Shan, Research progress on saponins, biological activities of saponins, and quality control of panax quinquefolium. China J. Chin. Materia Med. **47**, 36–47 (2022)
5. Y. Wang, H. Choi, J.A. Brinckmann, X. Jiang, L. Huang, Chemical analysis of panax quinquefolius (north American ginseng): a review. J. Chromatogr. A **1426**, 1–15 (2015)
6. B. Usman, N. Sharma, S. Satija, M. Mehta, M. Vyas, G.L. Khatik, N. Khurana, P.M. Hansbro, K. Williams, K. Dua, Recent developments in alpha-glucosidase inhibitors for management of type-2 diabetes: an update. Curr. Pharm. Des. **25**, 2510–2525 (2019)
7. G.B.D.D. Collaborators, Global, regional, and national burden of diabetes from 1990 to 2021, with projections of prevalence to 2050: a systematic analysis for the global burden of disease study 2021. Lancet. **402**, 203–234 (2023)
8. L. Han, L. Zhang, W. Ma, D. Li, R. Shi, M. Wang, Proanthocyanidin b_2 attenuates postprandial blood glucose and its inhibitory effect on alpha-glucosidase: analysis by kinetics, fluorescence spectroscopy, atomic force microscopy and molecular docking. Food Funct. **9**, 4673–4682 (2018)
9. H. Wang, J. Wang, Y. Liu, Y. Ji, Y. Guo, J. Zhao, Interaction mechanism of carnosic acid against glycosidase (α-amylase and α-glucosidase). Int. J. Biol. Macromol. **13**, 8846–8853 (2019)
10. U. Hossain, A.K. Das, S. Ghosh, P.C. Sil, An overview on the role of bioactive alpha-glucosidase inhibitors in ameliorating diabetic complications. Food Chem. Toxicol. **145**, 111738 (2020)
11. J. Xu, S. Wang, T. Feng, Y. Chen, G. Yang, Hypoglycemic and hypolipidemic effects of total saponins from stauntonia chinensis in diabetic db/db mice. J. Cell. Mol. Med. **22**, 6026–6038 (2018)
12. H. Wu, T. Liu, W. Wang, J. Feng, H. Tian, Oleanane-type saponins from the roots of ligulariopsis shichuana and their α-glucosidase inhibitory activities. Molecules. **22**, 1981 (2017)

13. H. Zhang, J. Xu, M. Wang, X. Xia, R. Dai, Y. Zhao, Steroidal saponins and sapogenins from fenugreek and their inhibitory activity against α-glucosidase. Steroids. **161**, 108690 (2020)
14. J. Lee, M. Choi, K. Seo, J. Lee, H. Lee, J. Lee, M. Kim, M. Lee, Platycodi radix saponin inhibits α-glucosidase in vitro and modulates hepatic glucose-regulating enzyme activities in c57bl/ksj-db/db mice. Arch. Pharm. Res. **33**, 773–782 (2013)
15. Y. Zhang, W. Tian, Y. Lu, Z. Li, D. Ren, Y. Zhang, J. Sha, X. Huo, S. Li, Y. Sun, American ginseng with different processing methods ameliorate immunosuppression induced by cyclophosphamide in mice via the mapk signaling pathways. Front. Immunol. **14**, 1085456 (2023)
16. X. Huang, Y. Liu, Y. Zhang, S. Li, H. Yue, C. Chen, S. Liu, Multicomponent assessment and ginsenoside conversions of panax quinquefolium l. roots before and after steaming by hplc-msn. J. Ginseng Res. **43**, 27–37 (2019)
17. N. Guo, Y. Bai, X. Huang, X. Liu, G. Cai, S. Liu, Y. Guo, J. Gong, Comparison of the saponins in three processed American ginseng products by ultra-high perfor-mance liquid chromatography-quadrupole orbitrap tandem mass spectrometry and multivariate statistical analysis. Int. J. Anal. Chem. 2022, 6721937 (2022)
18. C. Wang, H.H. Aung, M. Ni, J. Wu, R. Tong, S. Wicks, T. He, C. Yuan, Red American ginseng: ginsenoside constituents and antiproliferative activities of heat-processed panax quinquefolius roots. Planta Med. **73**, 69–674 (2007)
19. Y. Liu, J. Deng, D. Fan, Ginsenoside Rk_3 ameliorates high-fat-diet/streptozocin induced type 2 diabetes mellitus in mice via the ampk/akt signaling pathway. Food Funct. **10**, 2538–2551 (2019)
20. J.M. Kim, C.H. Park, S.K. Park, T.W. Seung, J.Y. Kang, J.S. Ha, D.S. Lee, U. Lee, D. Kim, H.J. Heo, Ginsenoside re ameliorates brain insulin resistance and cognitive dysfunction in high fat diet-induced c57bl/6 mice. Food Chem. **65**, 2719–2729 (2017)
21. Y. Lin, Y. Hu, X. Hu, L. Yang, X. Chen, Q. Li, X. Gu, Ginsenoside Rb_2 improves insulin resistance by inhibiting adipocyte pyroptosis. Adipocyte. **9**, 302–312 (2020)
22. X. Du, X. Wang, X. Yan, Y. Yang, Z. Li, Z. Jiang, H. Ni, Hypoglycaemic effect of all-trans astaxanthin through inhibiting α-glucosidase. J. Funct. Foods**74** (2020)
23. Y. Qiao, J. Nakayama, T. Ikeuchi, M. Ito, T. Kimura, K. Kojima, T. Takita, K. Yasukawa, Kinetic analysis of inhibition of α-glucosidase by leaf powder from morus australis and its component iminosugars. Biosci. Biotech. Bioch. **84**, 2149–2156 (2020)
24. A. Adalaiti, Z. Rui, Z. Yewei, T. Huiwen, Y. Junlin, B. Subinuer, M. Xiaoli, Identification of α-glucosidase inhibitors from mulberry using UF-UPLC-QTOF-MS/MS and molecular docking. J. Funct. Foods. **101**, 105362 (2023)
25. A.N. Qi, G. Mei, S. Ya-Jun, Z. Ying, W. Rui-Luan, G. Long, Z. Yu-Guang, Z. Dan, Comparative study on changes of ginsenosides and activities of American ginse-ng before and after steaming. China J. Chin. Materia Med. **4**, 4404–4410 (2020)
26. W. Huairui, C. Yao, Z. Xue, W. Yingping, Z. Hui, Comparative analysis of physi-cochemical properties, ginsenosides content and α-amylase inhibitory effects in white ginseng and red ginseng. Food Sci. Hum. Well. **12**, 14–27 (2022)
27. J. Shao, J. Jiang, J. Zou, M. Yang, F. Chen, Y. Zhang, L. Jia, Therapeutic potential of ginsenosides on diabetes: from hypoglycemic mechanism to clinical trials. J. Funct. Foods. **64**, 103630 (2020)
28. R. Zhou, D. He, J. Xie, Q. Zhou, H. Zeng, H. Li, L. Huang, The synergistic effects of polysaccharides and ginsenosides from American ginseng (Panax quinquefolius L.) ameliorating cyclophosphamide-induced intestinal immune disorders and gut barrier dysfunctions based on microbiome-metabolomics analysis. Front. Immunol. **12**, 665901 (2021)
29. G. Jia, J. Zhang, L. Han, Y. Zheng, Anti-obesity effect of saponins from stems and leaves of Panax Quinquefolium. Nat. Prod. Res. Dev. **17**, 3 (2005)
30. N.R. Kokila, B. Mahesh, R. Ramu, K. Mruthunjaya, B.K. Bettadaiah, H. Madhyastha, Inhibitory effect of gallic acid from thunbergia mysorensis against alpha-glucosidase, alpha-amylase, aldose reductase and their interaction: inhibition kinetics and molecular simulations. J. Biomol. Struct. Dyn. **41**, 10642–10658 (2022)